Durability of Fly Ash Geopolymer Concrete in a Seawater Environment

Monita Olivia[1] and Hamid R Nikraz[2]
[1]PhD student at Department of Civil Engineering, Curtin University, Perth, Western Australia, 6102, Australia
[2]Professor at Department of Civil Engineering, Curtin University, Perth, Western Australia, 6102, Australia

Synopsis: This paper presents the results of a study on the durability of fly ash geopolymer concrete in a seawater environment. In this research, three different geopolymer mixes and a control mix were examined to determine the effective porosity, chloride ion penetration, and corrosion of steel reinforcement bars under open circuit potential and accelerated corrosion tests. High chloride ingress was observed on the geopolymer paste. A depassivation of the passive film of the steel reinforcement bar in fly ash geopolymer was faster than for the OPC concrete. Small corrosion activities were conversely evident in the geopolymer concrete under the accelerated corrosion test at an applied voltage of 30 V. Decreased corrosion rates were observed for the geopolymer concrete. The results obtained from these tests indicate that the nature of the geopolymer paste certainly influences its durability in the seawater environment.

Keywords: chlorides, concrete, corrosion, fly ash, geopolymer

1. Introduction

Geopolymer is a new binder, which is produced by the reaction of an aluminosilicate material with an alkaline solution (1). Because it is high in silica and alumina slag, fly ash became an increasingly popular source material. It was chosen instead of metakaolin as the main material for the geopolymerisation process. Since slag and fly ash are by-products, they are abundantly available in landfill (2-4). However, fly ash is a heterogeneous material with a different chemical composition from metakaolin and that could affect the final geopolymer product (5). Nonetheless, low calcium fly ash is preferable to high calcium because there is a reduced risk of fast setting, which occurs when a mixture has a high calcium content. The parameters affecting the fly ash geopolymer mixtures include its raw materials, alkaline activators concentration, and curing method. A combination of sodium silicate (Na_2SiO_3) and sodium hydroxide (NaOH) as alkaline activators were used (6, 7); consequently, the ratio of sodium silicate to sodium hydroxide is significant when designing the mixtures. Furthermore, since fly ash has a slow reactivity in ambient temperatures, a high temperature is essential to increase the kinetics and degree in the reaction of the geopolymer process, to develop a denser pore system, and to produce good mechanical properties (8).

A number of studies have previously highlighted the strength properties and durability in aggressive environments such as sulphate (9), acid (10), and fire (11). Low calcium content could be an explanation for the resistance of fly ash in environments where calcium, which is a major element in Portland cement, has reacted with the aggressive ions. However, there is little literature concerning the durability of fly ash geopolymer concrete in a seawater environment. The present research focuses on the durability of fly ash geopolymer mixtures in seawater. The mixture optimization was carried out using the Taguchi method. Both the mechanical properties and the durability of the optimum mixtures were investigated.

2. Materials and Method

The fly ash geopolymer concrete was manufactured from fly ash, chemical solution, aggregates, and superplasticizer. The fly ash class F (ASTM C618), obtained from the Collie Power Station, Western Australia and Ordinary Portland Cement Type I (AS 2350) were used as the main materials. The chemical composition of the fly ash and cement are presented in Table 1. Coarse and fine aggregates in saturated surface dry conditions were used in this research. Crushed granite (with grain sizes of 7 mm, 10 mm, and 20 mm) and uncrushed sand dune were obtained from local quarries. The coarse aggregates have specific gravities of 2.65, 2.62, and 2.58; and water absorption of 0.58, 0.74, and 1.60% for the diameters 20 mm, 10 mm, and 7 mm, respectively. A combination of sodium hydroxide and sodium silicate was used as alkaline activators in the testing. Sodium hydroxide, in the form of pearl, was dissolved in distilled water to produce a sodium hydroxide solution with a 14 M concentration. Sodium

silicate with a specific gravity of 1.52 and a modulus silicate ratio (*Ms*) of 2 (where *Ms* = SiO_2/Na_2O, Na_2O = 14.7%, SiO_2 = 29.4%) was used in the preparation of alkaline activators. A commercially available naphthalene sulphonate polymer-based superplasticizer was included in the mixture.

Table 1 Chemical composition of fly ash and cement (%)

Oxides	Fly ash	Cement
Silica (SiO_2)	50.50	21.10
Alumina (Al_2O_3)	26.57	4.70
Calcium Oxide (CaO)	2.13	63.80
Ferric oxide (Fe_2O_3)	13.77	2.80
Potassium oxide (K_2O)	0.77	-
Magnesium oxide (MgO)	1.54	2.00
Sodium oxide (Na_2O)	0.45	0.50
Phosporus pentoxide (P_2O_5)	1.00	-
Sulphuric anhydride (SO_3)	0.41	2.50
Loss on ignition (LOI)	0.60	2.10
Chloride	-	0.01

Table 2 shows details, obtained from an optimization study (12), of the proportions used for the geopolymer concrete mixture. Three different optimum mixtures were proposed with a target compressive strength higher than 55 MPa at 28 days. The proportions were determined using the standard calculation for the design of fly ash geopolymer concrete, which was developed at Curtin University (13). An adjustment was made by adding extra water to attain the target strength rating.

Table 2 Optimum mixture proportions

Mixtures	Unit weight (kg/m^3)						
	Fly ash	Cement	Total aggregate	NaOH 14M	Sodium Silicate	SP	Water
OPC	-	422.3	1788.3	-	-	-	190
T4	461.5	-	1800.0	46.2	92.3	6.9	18.6
T7	424.6	-	1848.0	36.4	90.9	6.4	17.9
T10	498.5	-	1752.0	42.7	106.7	7.5	18.8

SP: Superplasticizer

The geopolymer and the OPC concrete specimens were cured using different methods. The geopolymer specimens were steam cured with three different curing regimes. These three curing methods: 24h–60^{O}C, 12h–70^{O}C, and 24h–75^{O}C were adopted from various authors (5, 12, 14). The moulds for geopolymer specimens were coated a with water-based release agent to prevent the samples from sticking to the moulds during the steam curing process. After demoulding, the specimens were left to air cure in the curing room with a temperature of 23–25^{O} C. The OPC specimens were demoulded after 24 hours and placed in the water pond for 28 days. The OPC specimens were then removed from the ponds and left to dry in the curing room until the testing date.

The specimens were cast in 100 x 200 mm cylinders for compressive strength, 150 x 300 mm for splitting tensile strength test, and 100 x 50 mm for both AVPV and effective porosity tests. Lollipop specimen bars of 100 x 200 mm with a 16 mm diameter were positioned in the centre of the concrete for the half-cell potential and accelerated corrosion tests. Three specimens were produced for each test and the results were reported as the average of three specimens. All specimens were tested on fresh properties, strength, and durability. The slump test was carried out in accordance with the Australian Standard (AS 1012.3.1-1998). The strength properties were determined by compressive strength (AS 1012.9-1999) and splitting tensile strength (AS 1012.10-2000). The Apparent Volume of Permeable Voids and effective porosity were measured using ASTM C642. The effective porosity was determined as follows:

Effective porosity (%) = (B-A)/V x 100 (1)

where A = mass of oven dried sample in air, B = saturated mass of the surface dry sample in air after immersion, V = bulk volume of the sample.

The chloride ion penetration was determined by the NTBuild 443 Test (15). To study the corrosion resistance of steel bars in fly ash geopolymer concrete, a half-cell potential measurement (ASTM C876-09) and an accelerated corrosion test (16) were both conducted. In this accelerated corrosion technique, the concrete specimens were immersed in 3.5% NaCl solution—the specimens were the anode. By applying a constant potential of 30 V to the system from a DC power supply—the external stainless steel plate was used as the cathode. Figure 1 shows the accelerated corrosion configuration used in this research.

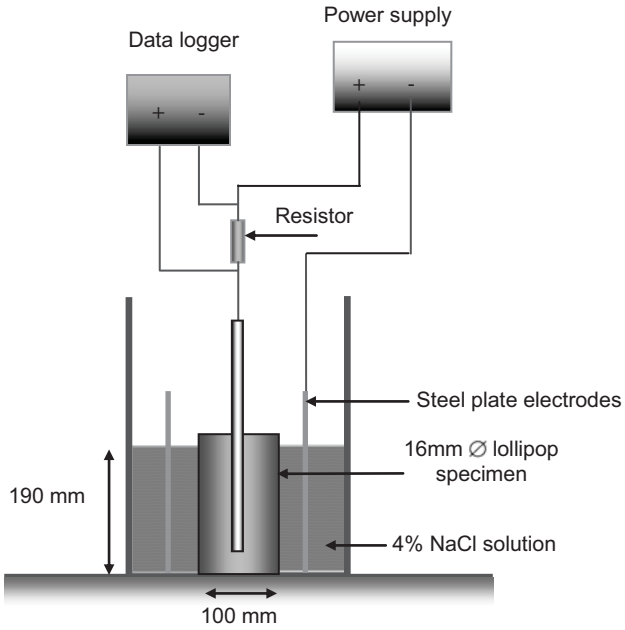

Figure 1 The accelerated corrosion set up (16).

After the corrosion test was completed, the rusty bars were cleaned with a wire brush. The percentage of corrosion mass loss was determined as the difference between initial and final mass of the steel bar. The mass loss can be used to calculate the corrosion rate of the steel bar after 91 days immersion in NaCl solution. The corrosion rate, which is based on steel mass loss, can be calculated according to ASTM G1(17):

Corrosion rate = (K x W)/(A x T x D) (2)

where K = a constant (see clause 8.1.2 ASTM G1), T = time of exposure (hours), A = area (cm^2), W = mass loss (grams) and D = density (g/cm^3, from Appendix X1 ASTM G1).

The original mass loss for specimens exposed in the accelerated corrosion test were recorded as the procedure given in ASTM G1 (17). The theoretical mass loss was calculated based on Faraday's Law as follows:

$\Delta w = (AIt)/ZF$ (3)

where: A = atomic weight of iron (56 grams), I = corrosion current (amp), t = time elapsed (seconds), Z = the valency of the reacting electrode (2 for iron), F = Faraday's constant (96,500 amp-sec).

3. Results and Discussion

3.1 Compressive and tensile strength

Table 3 displays the compressive strength of fly ash geopolymer concrete after 28 and 91 days of age. It is found that the compressive strength increases for mixes OPC, T7, T4, and T10 by 6.4%, 0.035%, 4.6%, and 5.1%, respectively. The OPC is showing a higher compressive strength than the fly ash geopolymer concrete. The steady increase in strength was assumed to be due to a slow reaction in refilling the gel structure and developing crystalline in the fly ash geopolymer system (18). On the other hand, mix T7

developed a minor strength gain after 28 days. This mix has a high aggregate content and less alkaline activator than was needed to react with the available silica and alumina from the fly ash, which may delay the increase of compressive strength. The same behaviour was observed for mixtures with a small amount of alkaline activators in the geopolymer fly ash mixed with rice husk ash (19). In this research, all of the tested mixes satisfied the AS3600 requirement for concrete in a seawater environment with a higher requisite compressive strength than 50 MPa at 28 days.

Table 3 Compressive strength (f'_c) and splitting strength (f_t) of concrete

Mixtures	Compressive strength (28 days)		Compressive strength (91 days)		Splitting strength (28 days)		Splitting strength (91 days)	
	f'_c (MPa)	SD	f'_c (MPa)	SD	f_t (MPa)	SD	f_t (GPa)	SD
OPC	56.22	1.63	59.86	4.88	3.97	0.49	4.25	0.13
T7	56.49	1.28	56.51	0.78	4.13	0.07	4.18	0.34
T4	56.24	4.45	58.85	3.48	3.96	0.16	4.10	0.19
T10	60.20	5.40	63.29	5.62	4.29	0.32	4.79	0.33

Table 3 additionally displays the splitting tensile strength for all of the mixes at 28 and 91 days. The splitting tensile strength of fly ash geopolymer concrete increased with the concrete's age. Mix T10 demonstrated higher tensile strength (11.6%) than the OPC concrete (7.1%). An effective bonding between the geopolymer matrix and the interface of aggregates may cause this (20). The high splitting tensile strength demonstrated by the mix T10 is advantageous as it decreases the rate and extent of cracking due to the corrosion of reinforcement (21).

3.2 AVPV and effective porosity

The AVPV and effective porosity of all of the concrete compounds are shown in Figure 2. It is observed that the AVPV and effective porosity for geopolymer concrete is found to be less when compared to the control concrete. Both mix T7 and T10 had porosity lower than 10% when compared to T4.

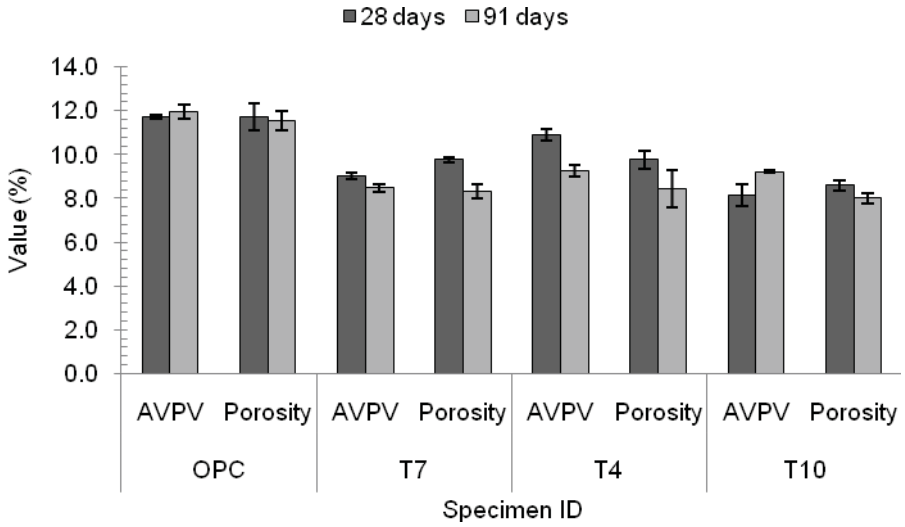

Figure 2 AVPV and effective porosity of OPC and geopolymer concrete at 28 and 91 days.

3.3 Chloride ion penetration

The chloride content of the specimens at a depth of 0–5 mm, 15–30 mm, and 30–45 mm from the NT Build 443 test are presented in Figure 3. The OPC concrete displayed a high chloride content value with a sharp decrease for the 30–45 mm concrete depth. A chloride resistant concrete is usually less susceptible to chloride as the depth increases. The geopolymer concrete showed the same trend for all

cover depths. The chloride content at a depth of 0–15 mm was quite high. The geopolymer concrete had a high chloride content with a range of 0.35–0.46% at a depth of 0–15 mm. There was a reduction of chloride content at a depth of 15–30 mm, with a range of 0.28–0.35%. The chloride content of the geopolymer concrete at a depth of 30–45 mm was 0.22–0.27%. The lowest chloride concentration among the geopolymer mixes was performed by T7.

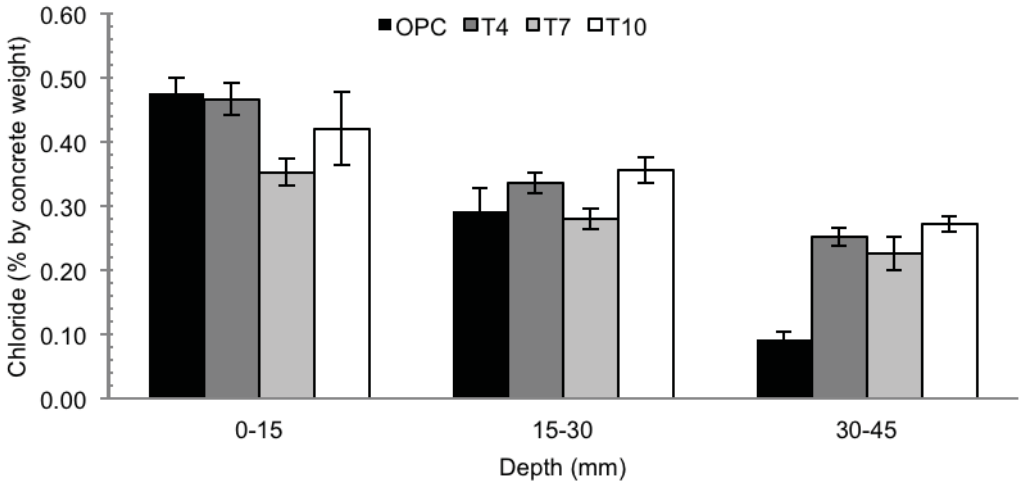

Figure 3 Chloride ion penetrations for depth of 0-15mm, 15-30mm and 30-45mm.

It can be seen that there are two probable reasons for the high chloride concentration in the geopolymer matrix. First, the fly ash geopolymer concrete with low calcium content has no C_3A that could enable a chloride binding mechanism to minimize direct chloride ion penetration of the concrete paste. The chloride binding ability of the OPC concrete is important to minimizing the chloride ion penetration (22). Second, there is no continuous hydration mechanism, such as in the OPC concrete, for the geopolymer paste immersed in an aqueous medium. Continuous hydration for concrete under water is beneficial to reduce porosity and further ingress from harmful ions such as chloride.

3.4 Corrosion by half-cell potential measurement

The half-cell potential measurement was carried out by an Ag/AgCl reference electrode for lollipop samples in a 3.5% NaCl solution. The reading is an average of the three specimens and a triplicate reading was taken for each sample as is shown in Figure 4.

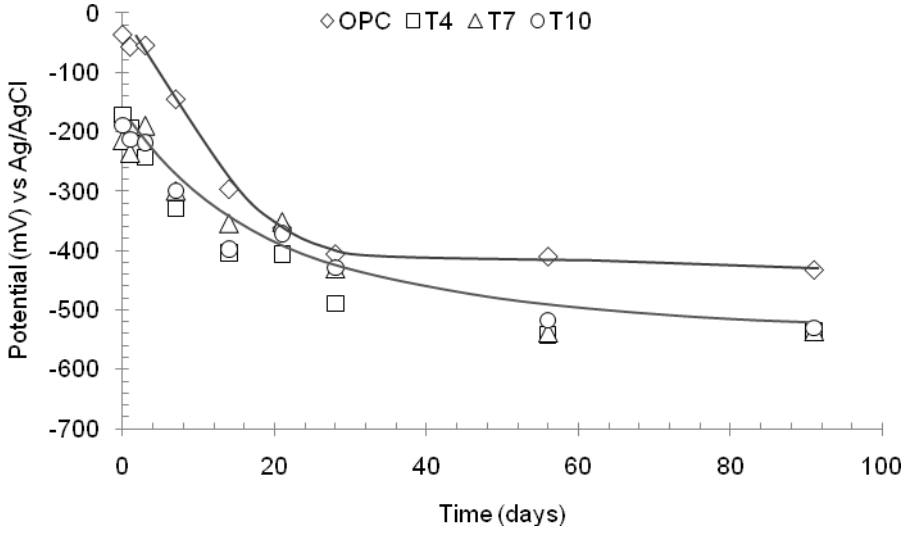

Figure 4 Change in half-cell potentials with respect to time.

All geopolymer concrete showed a greater negative corrosion potential of more than -500 mV vs. Ag/AgCl at 91 days. According to ASTM C876, the corrosion potential of less than -404 mV vs. Ag/AgCl, the concrete is predicted in severe corrosion (23). It appears that a high penetration of chloride ion into the concrete was the main cause of such a drop in the corrosion potential reading. The corrosion potential of the OPC concrete was also constant at -404 mV vs. Ag/AgCl at 91 days, clearing showing that the steel bars were also undergoing active corrosion.

Table 4 shows the average steel bar mass loss, corrosion mass loss, and the corrosion rate of OPC and geopolymer concrete specimens. The percentage of corrosion mass loss was determined as being the difference between initial and final mass. As can be seen from the table, the mass loss and, subsequently the corrosion rate of the geopolymer were generally lower than for the OPC concrete. The corrosion rates obtained for geopolymer are about 48 to 97 times lower than for OPC concrete. The OPC concrete had corrosion rates higher than 0.1016 mm/year or 'very high' according to the assessment criteria from Bertolini (24). Mix T10 showed corrosion rates between 0.0101–0.0500 mm/year, which comes under the category 'intermediate', while T4 and T7 performed corrosion rates of 0.102 and 0.260 mm/year, respectively, according to the same assessment criteria this comes under 'high'. This figure also clearly indicates that the type of binder certainly influences the corrosion rate of all mixtures. The improved corrosion resistance of fly ash geopolymer concrete could be due to the sodium silicate inclusion in the system, which acts like a corrosion inhibitor (25) and that can decrease the corrosion rate of steel reinforcement. More research is needed to investigate the corrosion inhibition effect and the corrosion product of the fly ash geopolymer concrete.

Table 4 Steel bar mass loss and corrosion rate

Mixtures	Initial weight (g)	Mass loss		Corrosion mass loss		Corrosion rate	
		W (g)	SD	W (%)	SD	L (mm/year)	SD
OPC	539.34	3.87	0.341	0.717	0.061	2.573	0.178
T4	540.53	0.17	0.006	0.031	0.001	0.102	0.009
T7	535.30	0.42	0.080	0.079	0.014	0.260	0.055
T10	539.31	0.04	0.010	0.007	0.002	0.025	0.006

3.5 Corrosion by impressed voltage method

Figure 5 displays the impressed voltage of 30 V test results of OPC and the various mixes of fly ash geopolymer concrete.

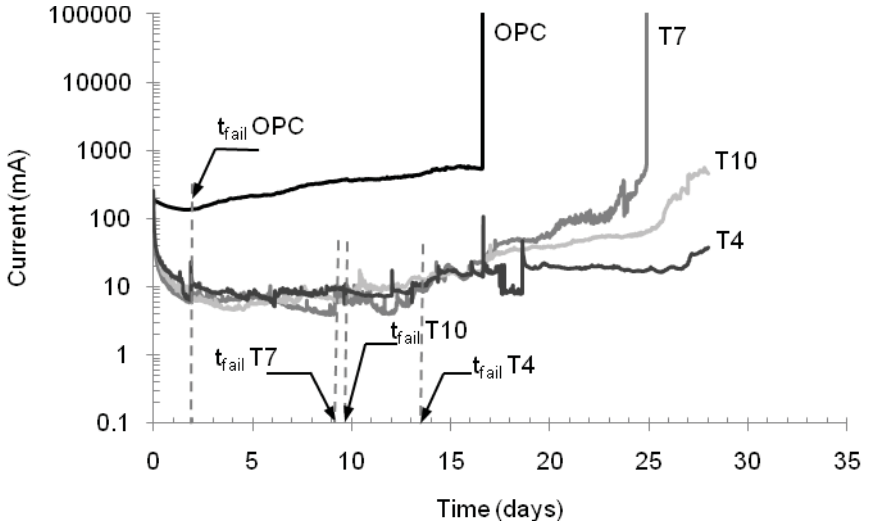

Figure 5 Corrosion current-time relationships of concrete at constant voltage of 30V.

In this test, the fly ash geopolymer concrete performed at a smaller current output rate than the OPC concrete. Before the specimens reached active corrosion potentials and cracked under impressed voltage, there was a gradual increase in the currents for the OPC concrete. According to previous researchers (27, 28), the recorded current of the geopolymer was always smaller than that of the OPC binder, which closely aligns with these findings. It was suggested that the type of binder influences the corrosion resistance, which is noted by the low current output.

The summary of corrosion current and time to failure values is presented in Table 5. Both types of concrete have notable differences for the initial and final current levels. In this research, at the time the specimens reach active corrosion potentials and crack under impressed voltage, the maximum currents that can be sustained by the set up was set at 10 Amps (99999.99 mA). The time to failure (t_{fail}) for both types of concrete specimens is defined as time corresponding to the onset of a large increase in currents (29). This data was determined by observing a change of current for every specimen. The OPC, T7, T4, and T10 failed at 2.27, 8.77, 12.94, and 9.22 days, respectively. This indicates that the geopolymer binder could delay the effect of impressed voltage to accelerate the corrosion process, although it was obvious that the presence of chloride ions depassivated the protective film of the embedded steel bar faster than the OPC concrete.

Table 5 Current reading and time to failure of samples at constant voltage of 30V

Mix	Initial current (mA)	Final current (mA)	Time to failure (days)
OPC	163.64	99999.99	2.27
T7	218.04	99999.99	8.77
T4	259.87	38.14	12.94
T10	268.02	66.33	9.22

The variation of time to failure with tensile strength is displayed in Figure 6. Although the tensile strength of the geopolymer was more or less similar to that of the OPC concrete, the average time of failure was longer. This can prevent a sudden crack due to volume expansion of rust in the concrete pores. However, there is no specific correlation between specimen failure and tensile strength for the geopolymer concrete.

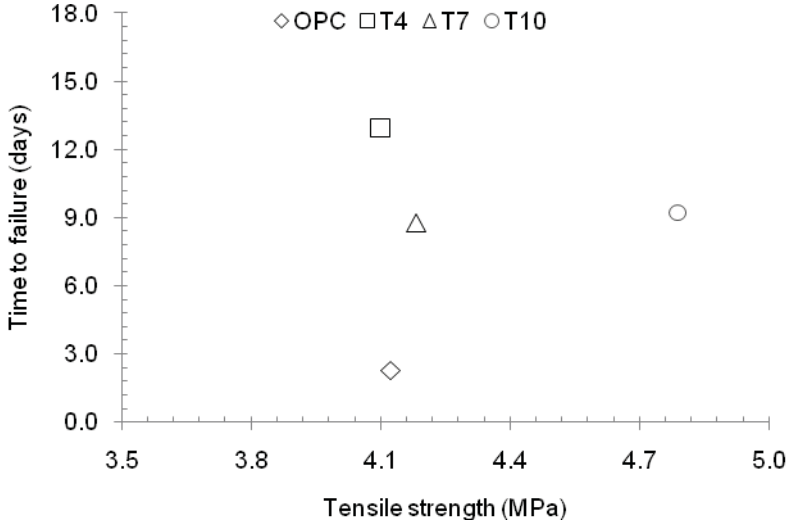

Figure 6 Variation of time to failure with tensile strength of concrete at 91 days.

4. Conclusions

The following conclusions can be drawn from this research.

1. The optimum fly ash geopolymer concrete has high compressive strength, tensile properties, and low effective porosity, which are all beneficial for concrete in a seawater environment.
2. The chloride ion penetration of fly ash geopolymer was higher than for the OPC concrete. In a seawater environment, there is a high risk of chloride-induced corrosion of steel reinforcement bars. This could be due to the absence of a chloride binding mechanism, such as in cement with C_3A, and lack of continuous hydration in the fly ash geopolymer to reduce porosity.
3. The corrosion potential of fly ash geopolymer and OPC was lower than -270 mV vs. Ag/AgCl at 91 days, which indicates a high risk of corrosion of the steel reinforcement bar. Based on the steel weight loss calculation, the fly ash geopolymer has a lower corrosion rate than the OPC concrete.
4. Although fly ash geopolymer concrete indicated severe corrosion under half-cell potential measurement, a minor corrosion activity and time to failure in relationship to the OPC concrete was observed under the accelerated corrosion test.

5. Acknowledgments

The authors wish to thank Gunawan Wibisono, Ashley Hughes, Jim Sherlock, Russell Wilkinson and Nhu Nguyen from SGS Laboratory for their contribution to laboratory works. Funding from Australian Development Scholarships for the first author's PhD study at Curtin University of Technology is gratefully acknowledged.

6. References

1. Davidovits, J., "Geopolymer: inorganic polymer new materials", Journal of Thermal Analysis, 37(8), 1991, pp 1633-1656.
2. Fernandez-Jimenez, A., Palomo, J.G. and Puertas, F., "Alkali-activated slag mortars: Mechanical strength behaviour", Cement and Concrete Research, 29(8), 1999, pp 1313-1321.
3. Cheng, T.W. and Chiu, J.P., Fire-resistant geopolymer produced by granulated blast furnace slag, Minerals Engineering, 16(3), 2003, pp 205-210.
4. ADAA Statistic Page [Internet], Wollongong: Ash Development Association of Australia, 2009, available from http://www.adaa.asn.au/statistics.htm.
5. van Jaarsveld, J.G.S., van Deventer, J.S.J., and Lukey, G.C., "The effect of composition and temperature on the properties of fly ash and kaolinite-based geopolymers", Chemical Engineering Journal, 89(1-3), 2002, pp 63-73.
6. Bakharev, T., "Geopolymeric materials prepared using Class F fly ash and elevated temperature curing", Cement and Concrete Research, 35(6), 2005, pp 1224-1232.
7. Hardjito, D., Wallah, S.E., Sumajouw, D.M.J., Rangan, B.V., "Fly ash-based geopolymer concrete", Australian Journal of Structural Engineering, 6(1), 2005, pp 77-84.
8. Kovalchuk, G., Fernandez-Jimenez, A., and Palomo, A., "Alkali-activated fly ash: Effect of thermal curing conditions on mechanical and microstructural development - Part II", Fuel, 86(3), 2007, pp 315-322.
9. Bakharev, T., "Durability of geopolymer materials in sodium and magnesium sulfate solutions", Cement and Concrete Research, 35(6), 2005, pp 1233-1246.
10. Song, X.J., Marosszeky, M., Brungs, M., and Munn, R., "Durability of fly ash based geopolymer concrete against sulphuric acid attack", Proceedings, 10DBMC International Conference on Durability of Building Materials and Components, Lyon, France, 17-20 April 2005.
11. Kong, D.L.Y., Sanjayan, J.G., and Sagoe-Crentsil, K., "Comparative performance of geopolymers made with metakaolin and fly ash after exposure to elevated temperatures", Cement and Concrete Research, 37(12), 2007, pp 1583-1589.
12. Hardjito, D., Wallah, S.E., Sumajouw, D.M.J., Rangan, B.V., "On the development of fly ash-based geopolymer concrete", ACI Materials Journal, 101(6), 2004, pp 467-472.
13. Rangan, B.V., "Low calcium fly ash based geopolymer concrete", Concrete Construction Engineering Handbook, E.G. Nawy, Editor. Taylor & Francis, 2008.
14. Shindunata, van Deventer, J.S.J., Lukey, G.C., and Xu, H., "Effect of curing temperature and silicate concentration on fly ash based geopolymerisation", Industrial & Engineering Chemistry Research, 45(10), 2006, pp 3559-3568.
15. Nord Test Build 443, "Concrete, Hardened: Accelerated Chloride Penetration", 1995, Espoo.

16. Güneyisi, E. and Gesoğlu, M., “A study on durability properties of high-performance concretes incorporating high replacement levels of slag”, Materials and Structures, 41(3), 2008, pp 479-493.
17. American Standard Testing of Material, “Standard Practice for Preparing, Cleaning, and Evaluating Corrosion Test Specimens (ASTMG1)”, 2003, ASTM International, Philadelphia.
18. Lloyd, R.R., “Accelerated ageing of geopolymers”, Geopolymers, Structure, Processing, Properties and Industrial Applications, J.L. Provis, J.S.J, van Deventer, Editors. Woodhead Publishing Limited, 2009.
19. Wongpa, J., Kiattikomol, K., Jaturapitakkul, C., Chindaprasirt, P., “Compressive strength, modulus of elasticity, and water permeability of inorganic polymer concrete”, Materials & Design, 31(10), 2010, pp 4748-4754.
20. Rangan, B.V., “Engineering properties of geopolymer concrete”, Geopolymers, Structure, Processing, Properties and Industrial Applications, J.L. Provis, J.S.J, van Deventer, Editors. Woodhead Publishing Limited, 2009.
21. Popovics, S., Simeonov, Y., Bozhinov, G. and Barovsky, N., “Durability of reinforced concrete in sea water”, Corrosion of Reinforcement in Concrete Construction, A.P., Crane, Editor, Ellish Harwood Limited, 1983.
22. Neville, A., “Chloride attack of reinforced concrete: an overview”, Materials and Structures, 28(2), 1995, pp 63-70
23. Masoud, S., and Soudki, K., “Evaluation of corrosion activity in FRP repaired RC beams”, Cement and Concrete Composites, 28(10), 2006, pp 969-977.
24. Bertolini, L., Elneser, B., Pedeferri, P., and Polder, R.B., “Corrosion of Steel in Concrete-Prevention, Diagnosis, Repair”, Wiley, 2004, Weinheim, Germany.
25. Yuan, M.-r., Lu, J.-t., and Kong, G. “Effect of SiO_2:Na_2O molar ratio of sodium silicate on the corrosion resistance of silicate conversion coatings”, Surface and Coatings Technology, 204(8), 2010, pp 1229-1235.
26. Lloyd, R.R., J.L. Provis, and J.S.J. van Deventer, “Pore solution composition and alkali diffusion in inorganic polymer cement”, Cement and Concrete Research, 40(9), 2010, pp 1386-1392.
27. Yodmunee, S., and Yodsujai, W., “Study on corrosion of steel bar in fly ash based geopolymer concrete”, Proceedings, International Conference on Pozzolan, Concrete and Geopolymer, Khon Kaen, Thailand, 24-25 May 2006.
28. Kriven, W.M., Gordon, M., Ervin, B.L., and Reis, H., “Corrosion protection assessment of concrete reinforcing bars with a geopolymer coating”, Proceedings, 30th International Conference on Advanced Ceramics and Composites, Daytona Beach, USA, 23-27 January 2006.
29. Florida Method, “Floride method of test for an accelerated laboratory method for corrosion testing of reinforced concrete using impressed current (FM 5-522)”, 2000, Florida.